

## Improved Symmetry Greatly Increases X-Ray Power from Wire-Array Z-Pinches

T. W. L. Sanford, G. O. Allshouse, B. M. Marder, T. J. Nash, R. C. Mock, R. B. Spielman, J. F. Seamen, J. S. McGurn, D. Jobe, T. L. Gilliland, M. Vargas, K. W. Struve, W. A. Stygar, M. R. Douglas, and M. K. Matzen  
Sandia National Laboratories, P.O. Box 5800, Albuquerque, New Mexico 87185

J. H. Hammer, J. S. De Groot, and J. L. Eddleman  
Lawrence Livermore National Laboratory, P.O. Box 808, Livermore, California 94550

D. L. Peterson  
Los Alamos National Laboratory, Los Alamos, New Mexico 87545-0010

D. Mosher  
Naval Research Laboratory, Pulsed Power Physics Branch, Washington, D.C. 20375

K. G. Whitney, J. W. Thornhill, P. E. Pulsifer, and J. P. Apruzese  
Naval Research Laboratory, Radiation Hydrodynamics Branch, Washington, D.C. 20375

Y. Maron  
Department of Nuclear Physics, Weizmann Institute, Rehovot 76100, Israel  
(Received 9 August 1996)

A systematic experimental study of annular aluminum-wire Z-pinches on a 20-TW electrical generator shows that the measured spatial characteristics and emitted x-ray power agree more closely with rad-hydro simulations when large numbers of wires are used. The measured x-ray power increases first slowly and then rapidly with decreasing interwire gap spacing. Simulations suggested that this increase reflects the transition from implosion of individual wire plasmas to one of an azimuthally symmetric plasma shell. In the plasma-shell regime, x-ray powers of 40 TW are achieved. [S0031-9007(96)01865-0]

PACS numbers: 52.55.Ez, 52.50.Dg, 52.50.Lp

Achieving on-axis cylindrical symmetry, i.e., perfect axial and azimuthal uniformity, in magnetically driven, high-current, Z-pinch implosions (Fig. 1) is an important element of plasma radiation source (PRS) load design similar to the spherical-symmetry requirement for inertial confinement fusion (ICF) pellet implosions [1]. The additional requirement of low mass at present current levels and pulse widths makes fabricating the ideal Z-pinch load challenging. Typically, masses less than  $500 \mu\text{g}/\text{cm}$  can be efficiently imploded on short-rise-time electrical generators such as the 20-TW Saturn accelerator [2]. The high-symmetry, low-mass tradeoff has led to the choice of gas puffs, thin foils, metal vapor jets, and low-density foams over cylindrical-wire arrays. Of these, only thin foils demonstrate similar peak power performance (30 TW) [3] to that reported on here, but they are difficult to fabricate and impractical for routine use on Saturn.

One-dimensional (1D) modeling of the implosion of thin plasma shells predicts much higher kilovolt x-ray powers and shorter pulses than had been seen experimentally using the loads mentioned above [4]. Such shells acquire radial kinetic energy (KE) from the magnetic pinch force when a high current flows axially through the shell. This energy is rapidly converted to x radiation when the

shell assembles and thermalizes on axis. The experiments described here are the first to approach some of the high-power, short-pulse-width characteristics of the 1D calculations.

Data and modeling [1,3–7] suggest that azimuthal and axial asymmetries related to the discreteness of individual wire plasmas and the manner in which they merge to form a plasma shell are partially responsible for reduced implosion quality compared to the 1D calculations. Implosion quality refers to the high radial compression required to (1) generate high x-ray power for

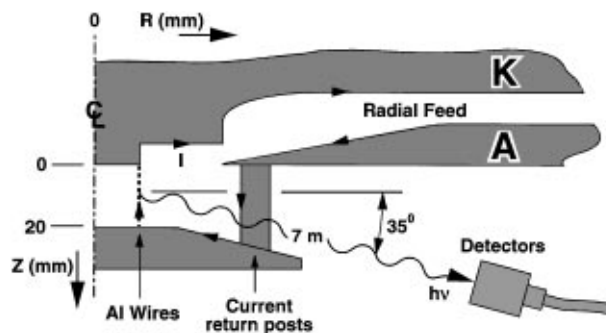


FIG. 1. Schematic cross section of experiment.

high-temperature *Hohlraums* used to provide Planckian radiation sources for ICF and high-energy-density experiments and (2) achieve excitation of high-atomic-number *K*-shell x rays for nuclear-radiation-effects studies. The experiments reported on here suggest that early formation of the plasma shell produced by increased wire number (reduced initial interwire gap) at constant total mass improves implosion quality. In these experiments, we systematically studied the dynamics of wire-array implosions as a function of wire number for two Saturn load geometries [8]. The intent was to determine if increasing load symmetry by increasing wire number would produce more symmetric and tighter pinches on axis. Aluminum wires were chosen for their large existing database, efficient radiation output, and availability of various wire diameters.

The experimental arrangement (Fig. 1) was similar to those previously employed [9], except for the number of wires in the array and diagnostic [8,10]. One load geometry consisted of 615- to 656- $\mu\text{g}$  arrays with  $N = 10$  to 136 wires on a mounting radius of  $R_i = 8.6$  mm, and the other consisted of 820- $\mu\text{g}$  arrays with  $N = 13$  to 192 wires on  $R_i = 12$  mm. These geometries covered initial interwire gaps  $G_i = 2\pi R_i/N$  of 6 to 0.4 mm. Eight current return posts were positioned at 17- and 27-mm radii for the small and large radius loads, respectively, with two or three *B*-dot load-current monitors at a 45-mm radius. For both geometries, 20-mm wire lengths were used. Typically, 7 MA with a 35-ns (10–90)% rise time flowed through the load (Fig. 2), corresponding to a calculated KE of 280 to 350 kJ carried by the imploding plasma when a 20:1 radial compression is achieved. A bolometer, arrays of filtered x-ray diodes and photoconducting detectors (PCDs) measured x-ray emission from 10 to 7000 eV. A time- and radius-resolved KAP crystal spectrometer covered 800 to 3500 eV. Two time-resolved x-ray pinhole cameras (PHCs) recorded x-ray images above 200 and

1000 eV. All radiation detectors were located about 7 m from the pinch in vacuum line of sights that viewed 70% of the pinch length at a 35° angle with respect to the normal to the pinch axis.

The improvement in pinch quality with wire number in both geometries is evident in x-ray PHC images and manifests itself as increased inductive current notches at peak compression (82 ns in Fig. 2), increased radial compression in the x-ray images, reduced radiation rise time and pulse width, and increased x-ray power. Figure 3 illustrates the reductions in rise time (from 48 to 2.3 ns) and pulse width (from 60 to 3.2 ns), and the associated increase in power (from 0.7 to 5 TW) of emitted *K*-shell x rays (energy greater than about 1 keV) as  $N$  is increased from 10 to 90 in the small-radius loads. For both loads, the radial compression improves from less than 10:1 for  $G_i = 6$  mm to more than 20:1 for  $G_i = 0.4$  mm. Over this range, the total radiated energy increases from  $\sim 175$  to  $\sim 350$  kJ for the small radius load and from  $\sim 240$  to  $\sim 440$  kJ for the large radius load. The peak values exceeded the calculated KE for a 20:1 compression by about 25%. When the various radiation characteristics are plotted versus  $G_i$ , as exemplified in Fig. 4 for the peak total power, the data for the two geometries fit a single curve dependent on gap alone. Here, as with the calculated KE, the systematic uncertainty due to calibration and response corrections is estimated to be  $\pm 15\%$ . Below  $G_i \approx 1.4$  mm, the increase in power with decreasing gap becomes rapid in all x-ray channels, suggesting a transition between two different kinds of implosion.

As shown by the total x-ray signal of Fig. 2, the 90-wire *K*-shell x-ray signal of Fig. 3, and the radial motion of time-resolved x-ray images [8,10], large- $N$  implosions exhibit a second, weaker compression/expansion predicted by 1D analysis [11]. For high-wire-number loads, measurements were compared with two, 2D *rz* RMHC simulations: a multi-photon-group Lagrangian code L-RMHC [12], and a three-temperature Eulerian code E-RMHC [13]. The codes used a circuit model of the Saturn accelerator coupled to the dynamic PRS load

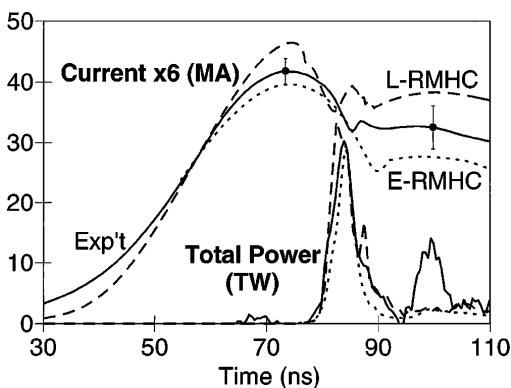


FIG. 2. Comparison of measured (solid) current and total power with Lagrangian radiation magnetohydrodynamic code (L-RMHC) (dashed line) and Eulerian radiation magnetohydrodynamic code (E-RMHC) (dotted line) for 8.6-mm radius and 90 wires. E-RMHC power shifted left by 6 ns.

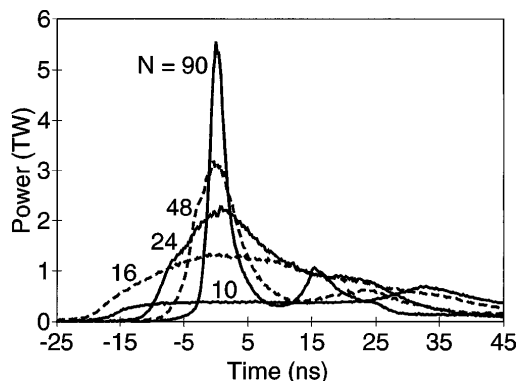


FIG. 3. *K*-shell power versus time for various wire numbers. Relative time shifts of 3 to 8 ns were applied to align peak-power times, defined to be zero.

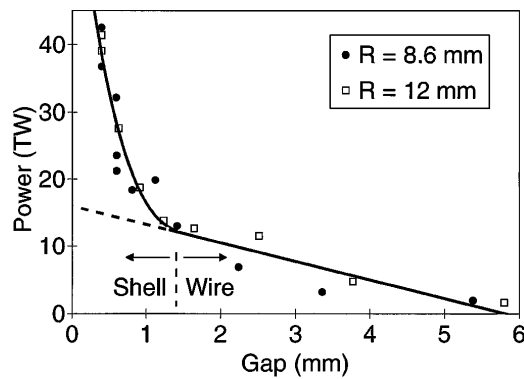


FIG. 4. Maximum total x-ray power versus initial wire gap.

that enabled peak currents to be calculated to the  $\pm 5\%$  accuracy of the experiment (Fig. 2).

Figure 2 demonstrates that the current and total x-ray power measured in high- $N$  loads can be reproduced by the  $r_z$  RMHCs. These calculations assumed small ( $\sim 5\%$ ) initial random density perturbations in an initial annular plasma that was  $\sim 1$  mm thick. Progressively larger initial perturbations are needed to reproduce the data as  $N$  decreases [12]. For both codes, radial compression is limited by magnetic Rayleigh-Taylor (RT) instabilities growing out of the initial perturbation. The main x-ray pulse begins when the RT bubble (inner radius of the unstable region [12,13]) reaches the axis, peaks, and ends when the spike (outer radius of the unstable region) finishes stagnating on axis. E-RMHC modeled the entire load length, producing a small second radiation peak at about the same time as the data (Fig. 2). In E-RMHC, 1-mm-wavelength RT modes grew during implosion, merged into 3-mm-wavelength modes, and seeded a 3-mm-wavelength sausage instability following peak compression, all of which are observed in x-ray images. In L-RMHC, the limited axial simulation length of 1 mm reproduced the short RT modes but prevented growth of the longer-wavelength ones. Analysis of the PHC images, PCD data, and  $K$ -shell spectra shows that near peak compression, the pinch is composed of a hot core ( $T_e \sim 1.3$  keV) surrounded by a cooler ( $\sim 0.4$  keV) plasma [10]. These results are in qualitative agreement with the  $r_z$  RMHC codes, although the codes predict emission localized to smaller radii than observed experimentally [14]. This discrepancy may be due to the 3D nature of the implosion and the code assumption of local thermodynamic equilibrium [12].

Using the measured current, including a 100-ns-long current prepulse shown in the inset of Fig. 5, a 1D L-RMHC was used to compute the radial dynamics of an isolated single-wire plasma from the solid state (Fig. 5). For a current-per-wire equivalent to that of  $N \leq 20$ , the expansion of an individual wire plasma is reversed by the self-magnetic field before the array implodes to the axis (labeled stagnation time in Fig. 5). For the lower current

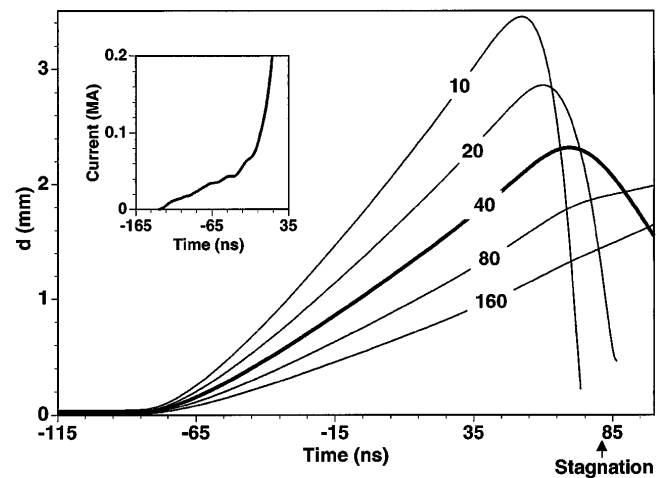


FIG. 5. Diameter of wire plasma versus time for various wire number, small-radius loads.  $t = 0$  corresponds to the arrival time of the main current pulse.

per wire when  $N \geq 80$ , the expansion would continue for longer than the implosion time. In these calculations, the dynamics is highly dependent on the resistivity model used. The early-time radial distributions from these calculations were then used as initial conditions for an  $xy$  RMHC [15] simulation of the array configuration in the  $r\theta$  plane (Fig. 6). These  $xy$  simulations showed that the 1D behavior of individual wire plasmas illustrated in Fig. 5 is not substantially altered in the array configuration. For our experiment at  $N = 40$  ( $G_i = 1.4$  mm), the expanding individual wire plasmas (Fig. 5) are calculated to merge with adjacent wire plasmas (Fig. 6) to form a continuous plasma annulus prior to implosion. For smaller  $N$ , individual wire plasmas do not merge during expansion because of the increased gap, and the self-pinching due to the high wire-plasma current. For larger  $N$ , a more symmetric annulus is formed by the densely packed, expanding wire plasmas. The more effective plasma merger with larger  $N$  (decreasing  $G_i$ ) helps explain the improvement in implosion quality for  $G_i$  less than 1.4. Moreover, the calculated transition between individual wire plasma and the continuous plasma-shell implosions at about 1.4 mm correlates with the observed transition between the slow and rapid variation in x-ray powers with decreasing  $G_i$  (Fig. 4).

The above analyses, however, are insufficient to elucidate the mechanisms responsible for the reduced implosion quality observed in the PHC images at small  $N$ , as even the discrete-wire implosions of  $N = 10$  in Fig. 6 display impressive radial compression. When  $N$  is small, large-amplitude sausage instabilities can grow as the individual wire plasmas self-pinch [7], forming axial asymmetries that are uncorrelated with their neighbors. Once unstable wire plasmas merge, the resulting 3D asymmetries represent a large perturbation for RT growth and contribute to low implosion quality, poor shot-to-shot

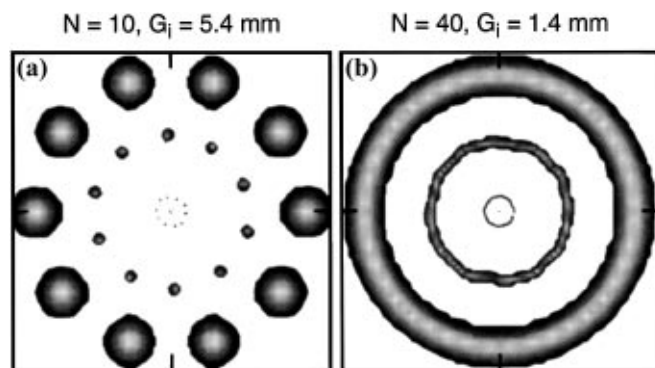


FIG. 6.  $xy$ -RMHC simulations for (a) 10- and (b) 40-wire, 8.6-mm implosions at 86, 11, 3, and 0 ns before stagnation. Azimuthal orientations at different times are not correlated.

reproducibility, and low radiated power. Both single-wire experiments and modeling of nonlinear sausage growth [7] show that some axial regions of pinched, unmerged wire plasmas will retain radial extents comparable to that at maximum expansion throughout the implosion, leading to stagnated-plasma radii much larger than shown in Fig. 6. Thus, both azimuthal asymmetry and wire-plasma sausage growth are required to explain the poor observed implosion quality in the large-gap regime. As  $N$  increases beyond 40, pinching and the associated large-scale sausage instabilities become less important. This physical picture supports the observed scaling of implosion quality with  $N$  and is consistent with fast-framing x-ray PHC measurements: For gaps as small as 1.4 mm, wires were seen to implode as separate entities until just before plasma assembly. High-power, small-gap shots showed, on the other hand, formation of well-defined plasma shells prior to stagnation.

In summary, we have shown that reducing initial azimuthal asymmetries, by decreasing the interwire gap in 8.6- to 12-mm-radius PRS loads, provides dramatic gains in radiated x-ray power with its limit seemingly not yet observed (Fig. 4). These data are permitting, for the first time with wire arrays, 2D  $rz$ -RMHC simulations to be compared in detail with experiment at much reduced levels of asymmetry and instability.

We thank W. Beezhold, J. Maenchen, D. H. McDaniel, J. J. Ramirez, A. Toor, J. Davis, M. E. Jones, C. Deeney, L. P. Mix, B. M. Henderson, B. P. Peyton, R. S. Broyles, L. O. Peterson, and the Saturn crew for their contributions and support. This work was supported by U.S. DOE Contract No. DE-AC04-94AL85000.

- 
- [1] N. R. Pereira and J. Davis, *J. Appl. Phys.* **64**, R1 (1988).
  - [2] D. D. Bloomquist *et al.*, in *Proceedings of the 6th IEEE Pulsed Power Conference Arlington, VA, 1987*, edited by B. H. Bernstein and P. J. Turchi (IEEE Publishing Services, New York), IEEE Cat. 87CH2522-1, p. 310.
  - [3] D. H. McDaniel (private communication).
  - [4] K. G. Whitney *et al.*, *J. Appl. Phys.* **67**, 1725 (1990); J. W. Thronhill *et al.*, *J. Quant. Spectrosc. Radiat. Transf.* **44**, 251 (1990); J. W. Thronhill *et al.*, *Phys. Plasmas* **1**, 321 (1994).
  - [5] K. G. Whitney *et al.*, in *Dense Z-Pinches*, edited by Malcolm Haines and Andrew Knight, AIP Conf. Proc. No. 299 (AIP, New York, 1994), p. 429.
  - [6] D. Mosher, in *Proceedings of the 10th International Conference on High Power Particle Beams, San Diego, 1994*, edited by W. Rix and R. White, NTIS PB95-144317, p. 159.
  - [7] D. Mosher and D. Colombant, *Phys. Rev. Lett.* **68**, 2600 (1992), and single-wire experiments reference therein.
  - [8] T. W. L. Sanford *et al.*, in *Proceedings of the 11th International Conference on High Power Particle Beams, Prague, Czech Republic, 1996* (to be published); *Bull. Am. Phys. Soc.* **4**, 1846 (1995).
  - [9] R. B. Spielman *et al.*, in *Dense Z-Pinches* (Ref. [5]), p. 404.
  - [10] T. W. L. Sanford *et al.*, *Rev. Sci. Instrum.* (to be published).
  - [11] D. Mosher, in *Dense Z-Pinches*, edited by Nino Pereira, Jack Davis, and Norman Rostoker, AIP Conf. Proc. No. 195 (AIP, New York, 1989), p. 191.
  - [12] J. H. Hammer *et al.*, *Phys. Plasmas* **3**, 2063 (1996).
  - [13] D. L. Peterson *et al.*, *Phys. Plasmas* **3**, 368 (1996); W. Matuska *et al.*, *Phys. Plasmas* **3**, 1415 (1996).
  - [14] T. W. L. Sanford *et al.*, (to be published).
  - [15] B. M. Marder, *Math Comput.* **29**, 434 (1975).